Transactions, SMiRT-22
San Francisco, California, USA - August 18-23, 2013
Division II

MODELING AND FATIGUE ANALYSIS OF BOLTED JOINTS OF THE REACTOR PRESSURE VESSEL

M.H.C. Hannink, F.J. Blom, and N. Madan

Safety & Power, Nuclear Research and consultancy Group (NRG), The Netherlands (hannink@nrg.eu)

ABSTRACT

The upper head and vessel of the reactor pressure vessel (RPV) of a pressurized water reactor are generally connected by bolts. Varying thermal and mechanical loading conditions, due to e.g. start-up, shutdown, and opening and closing of the vessel for refueling, can lead to considerable stress fluctuations in the materials. A proper assessment of the fatigue endurance of the bolts is therefore indispensable.

Design calculations of RPVs built in the previous century were often made using two-dimensional (2D) axisymmetric (or even more simplified) models. For long term operation of nuclear power plants (NPPs), usually new state-of-the-art fatigue analyses are required. Nowadays, full three-dimensional (3D) finite element (FE) techniques are available, allowing for comparison with existing 2D axisymmetric analyses. In this paper, the influence of 2D and 3D modeling of the flanges of the RPV on the fatigue assessment of the bolts is presented.

INTRODUCTION

Long term operation of NPPs generally requires an update of time limited ageing analyses (IAEA Safety Report Series No. 57, 2008). One of such analyses is the fatigue analysis of bolted joints of the RPV. Cyclic loadings of the these joints consist of fluctuating temperatures and internal pressures during the different load cases, and unloading/preloading during opening/closing of the RPV for refueling.

Due to limited computational power, in the past, design calculations were often made using two-dimensional (2D) axisymmetric (or even more simplified) models. Nowadays, available computational power allows for full 3D analyses. To assess and update time limited ageing analyses for long term operation, it is useful to have insight in the influence of 2D and 3D modeling techniques. Therefore, a comparison is made between 2D axisymmetric and 3D modeling techniques of bolted joints of the RPV.

The bolted connection of the upper head and the vessel of the RPV as presented in this paper was analyzed using the commercial FE program ANSYS. The flanges of the RPV were modeled in two different ways: 2D axisymmetrically and 3D. Cook et al. (2007) presented an extensive study on the influence of different modeling techniques of bolts. In both models presented in the current paper, one of these techniques was used. The bolts were modeled with beam elements and the heads of the bolts were simulated by a series of beam elements in a web-like fashion. The influence of the different modeling techniques of the flanges on the fatigue endurance of the bolts is demonstrated by comparing the cumulative usage factors (CUFs) of the bolts.

In the next sections, the geometry, materials, and finite element models are presented in more detail. Thereafter, the loading conditions and the approach for the fatigue assessment are discussed. Finally, results are presented and conclusions are drawn.

MODEL

Geometry

The geometry of the upper head, vessel and bolts of the RPV is shown in Figure 1.

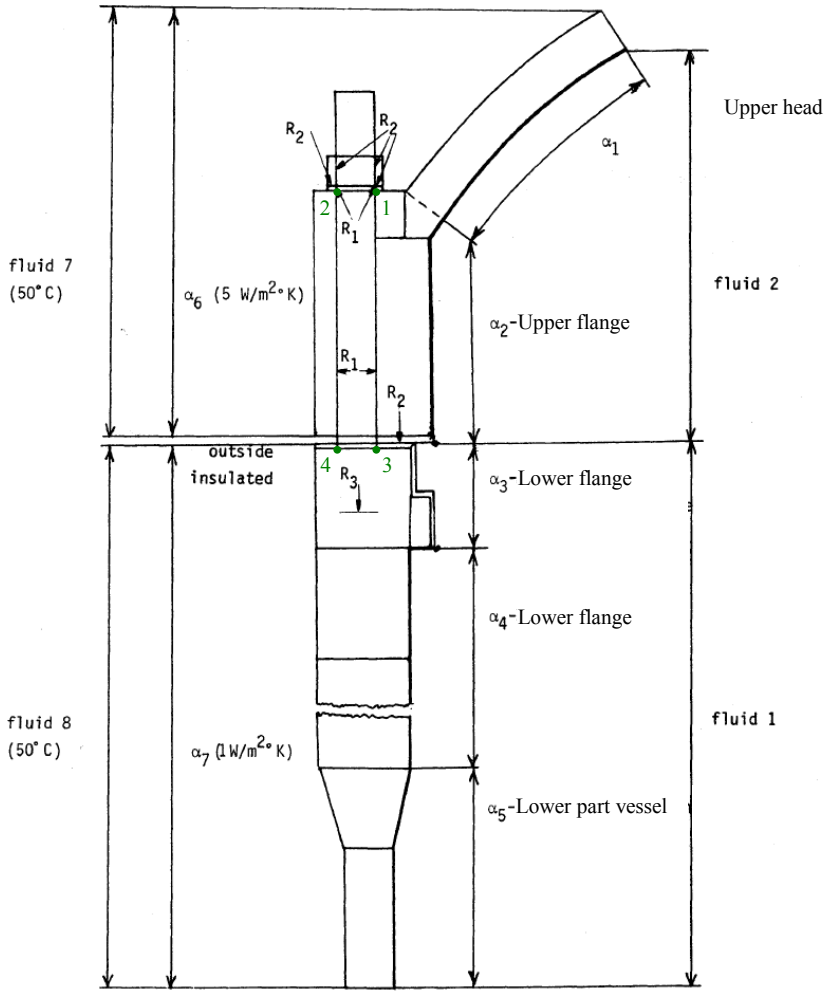

Figure 1. Bolted joint of RPV with convection boundary conditions and locations for fatigue evaluation.

Materials

The RPV is made of 22 Ni Cr Mo 37 steel and the bolts are made of ASME 540 Gr. B 24. At the parts where the upper head and the vessel are in contact, an X 10 Cr Ni Nb 189 austenitic steel cladding is present (see Figure 2). The temperature dependent material properties as used in the models are listed in Table 1 and Table 2, where T is the temperature, E is the Young's modulus, α is the thermal expansion coefficient, k is the thermal conductivity, and c_p is the specific heat at constant pressure. For the cladding, a density of 7900 kg/m^3 was used. For the flanges and bolts, a density of 7850 kg/m^3 was used. For all materials, a Poisson's ratio of 0.3 was taken.

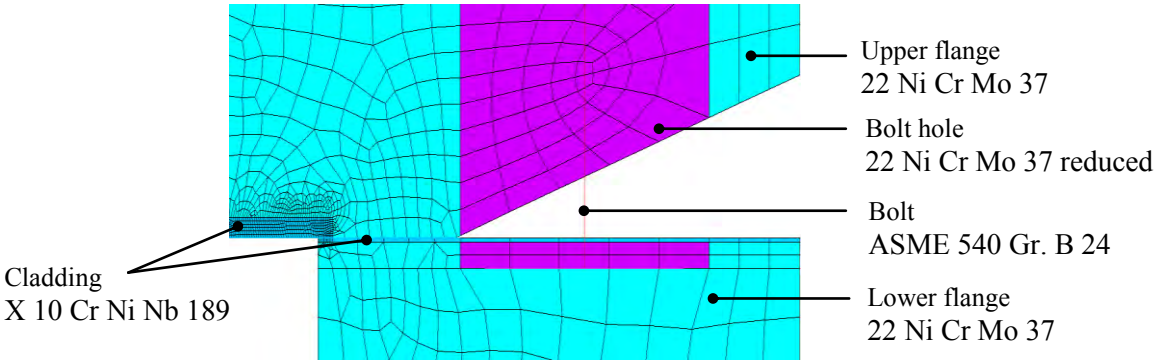

Figure 2. Materials in model (zoomed in on contact area of flanges).

Table 1: Material properties of 22 Ni Cr Mo 37 (flanges) and X 10 Cr Ni Nb 189 (cladding).

	22 Ni Cr Mo 37				X 10 Cr Ni Nb 189			
T [°C]	E [MPa]	α [K^{-1}]	k [Wm/K]	c_p [J/kgK]	E [MPa]	α [K^{-1}]	k [Wm/K]	c_p [J/kgK]
20	206010	$11 \cdot 10^{-6}$	45.8	459.87	199140	$15.3 \cdot 10^{-6}$	15.3	489.80
307	177560	$13 \cdot 10^{-6}$	40.4	551.60	171680	$17.1 \cdot 10^{-6}$	18.8	551.89
350	174618	$13 \cdot 10^{-6}$	39.6	569.40	166770	$17.3 \cdot 10^{-6}$	19.2	567.08

Table 2: Material properties of ASME 540 Gr. B 24 (bolts).

T [°C]	E [MPa]	α [K^{-1}]	k [Wm/K]	c_p [J/kgK]
20	206010	$10 \cdot 10^{-6}$	45.4	459.87
307	183450	$12 \cdot 10^{-6}$	40.3	551.60
350	176580	$12.3 \cdot 10^{-6}$	39.5	569.40

FINITE ELEMENT MODELING

Finite Element Models

The bolted joint was modeled using the commercial FE program ANSYS, version 12.1. First, the temperature distributions in the flanges and bolts were calculated by performing a transient thermal analysis. Subsequently, the resulting temperature distributions, internal pressure loading, and pretension in the bolts were applied in a mechanical analysis to obtain the stresses in the bolts. For both analyses, the same meshes were used.

The meshes of the 2D axisymmetric model and the 3D model are shown in Figure 3. The RPV is closed by a total of 45 bolts. Due to symmetry, the 3D model consists of a 4° slice of the RPV incorporating half a bolt. To make an appropriate comparison, the mesh (size) of both models was kept similar.

In both models, the bolts were modeled using beam elements. In the thermal analysis, the contact between the bolts and the flanges was simulated by coupling the temperature degree of freedom at the top

and bottom of the bolts to the flanges. In the mechanical analyses, the head and the thread were simulated by a series of stiff beam elements in a web-like fashion (see Figure 3). In a cold state, the bolts have a pretension of 4178 kN. This was modeled by prescribing an initial strain. In the 2D axisymmetric model, the value of the initial strain was chosen so that the bolt force was equal to 45 times the preload. The cross-sectional area and moment of inertia of the beam elements representing the bolt were taken representative for the cross-sectional areas and moments of inertia of 45 bolts. In the 3D model the cross-sectional area, moment of inertia, and bolt force were equal to the values of half a bolt.

The upper head and vessel were meshed with quadratic elements. In the 2D axisymmetric model, the effect of the bolt holes was taken into account by multiplying the Young's modulus and the thermal conductivity in that area by a reduction factor (see Figure 2). The contact between the upper and lower flanges was modeled using target elements and contact elements with a coefficient of friction of 0.15.

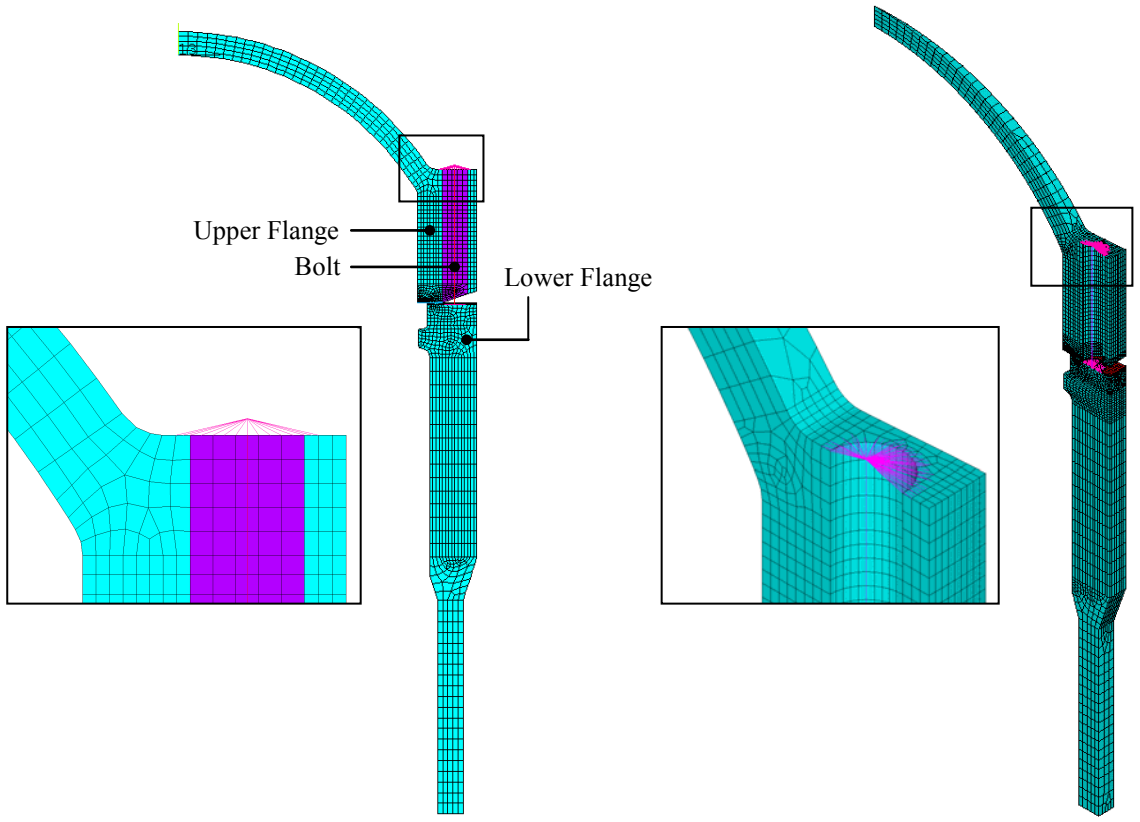

Figure 3. 2D axisymmetric (left) and 3D (right) FE models of bolted joint of RPV.

Boundary Conditions

The thermal boundary conditions at the outside of the RPV were simulated by prescribing a heat transfer coefficient of 1 W/m^2K at the outside of the vessel, a heat transfer coefficient of 5 W/m^2K at the outside of the upper head, and a fluid temperature of 50 °C (see Figure 1).

In the mechanical analysis, symmetry conditions were applied at the top of the upper head. The lower edge of the vessel was constrained by suppressing the displacements in axial direction. At both sides of the slice in the 3D model symmetry conditions were applied.

LOADING CONDITIONS

The stresses in the bolts are caused by both thermal and mechanical loading conditions. Thermal stresses are caused by variations in water temperature and heat transfer coefficients. Mechanical stresses are due to internal pressure and pretension in the bolts.

The thermal loading conditions are defined by a time dependent inlet temperature and a time dependent outlet temperature. The values of the heat transfer coefficients are dependent on the (time dependent) fluid velocity and the geometry of the structure through which the fluid flows. At the inner surface of the RPV, five zones with different heat transfer coefficients were distinguished (α in Figure 1). The values as used in the model were determined according to the Wärmeatlas (1984) and were ranging from 5 W/m^2K to 30,000 W/m^2K. Table 3 shows an overview of the load cases that were included in the fatigue analysis. Load cases 1-15 are transient load cases, and load cases 10-16 are steady-state load cases.

Table 3: Load cases for fatigue analysis.

Load Case	Description
1	Start-up
2	Shutdown
3	Power change 100% - 40% - 100%
4	Turbine trip
5	SCRAM
6	Steam generator pipe break
7	Failure of a pressurizer safety valve
8	Failure of a main steam safety valve
9	Pretension
10	Steady state
11	Pressure 175.5 bar
12	Pressure 84 bar
13	Pressure 165 bar
14	Pressure 152.5 bar
15	Zero load

FATIGUE ASSESSMENT

The temperature and stress results, obtained from the thermal and mechanical analyses, were used to calculate the CUFs of the bolts. The bolts of the RPV were assessed according to the KTA Safety Standards 3201.2, Section 7.8.3 (1996). For the fatigue analysis, twelve operational cycles were defined. Each operational cycle was defined by a number of consecutively acting load cases and a number of occurrences. The fatigue assessment was performed using the postprocessor of ANSYS, which is consistent with the KTA approach. The fatigue design curve for high strength steel bolting that was used is shown in Table 4.

CUFs were calculated at two locations in the bolt: the top and the bottom. For each location, results were obtained at two sides of the cross-section of the beam. For each location, therefore, also two CUFs were calculated. In accordance with KTA 3201.2, Section 7.12.2, the stress intensity ranges in the bolts were multiplied by a fatigue strength reduction factor of 4. The fatigue assessment was performed for an operation period of 40 years.

Table 4: Fatigue design curve for high strength steel bolting (KTA, June 1996).

Number of Cycles	$1 \cdot 10^1$	$2 \cdot 10^1$	$5 \cdot 10^1$	$1 \cdot 10^2$	$2 \cdot 10^2$	$5 \cdot 10^2$	$1 \cdot 10^3$	$2 \cdot 10^3$
S_a [MPa]	7930	5240	3100	2210	1550	986	689	490
Number of Cycles	$5 \cdot 10^3$	$1 \cdot 10^4$	$2 \cdot 10^4$	$5 \cdot 10^4$	$1 \cdot 10^5$	$2 \cdot 10^5$	$5 \cdot 10^5$	$1 \cdot 10^6$
S_a [MPa]	310	234	186	152	131	117	103	93.1

RESULTS

Temperature Distribution

Figure 4 shows the temperature distribution in the flanges and the bolts during start-up and shutdown. During the load cases that involve a temperature increase (e.g. start-up), the inner wall of the vessel is warmer than the outer wall. During load cases that involve a temperature decrease (e.g. shutdown), it is the other way around. A comparison of the calculated temperatures in the bolts is shown in Figure 5. The results are shown for the time steps that were included in the fatigue analysis.

During the increasing temperature transient (load case 1), the bolt temperature calculated with the 3D model is slightly higher than the temperature resulting from the 2D axisymmetric model (see Figure 4, left and center, and Figure 5). During decreasing temperature transients (load cases 2, 5-8), the bolt temperature resulting from the 3D model is slightly lower (see Figure 5). These trends can be explained by the way in which the bolt holes were modeled. The flanges with the bolt holes (3D model) allow for more (local) heat conduction from the inner wall of the vessel to the outer wall than the flanges with the areas with reduced conductivity (2D axisymmetric model) (see Figure 4).

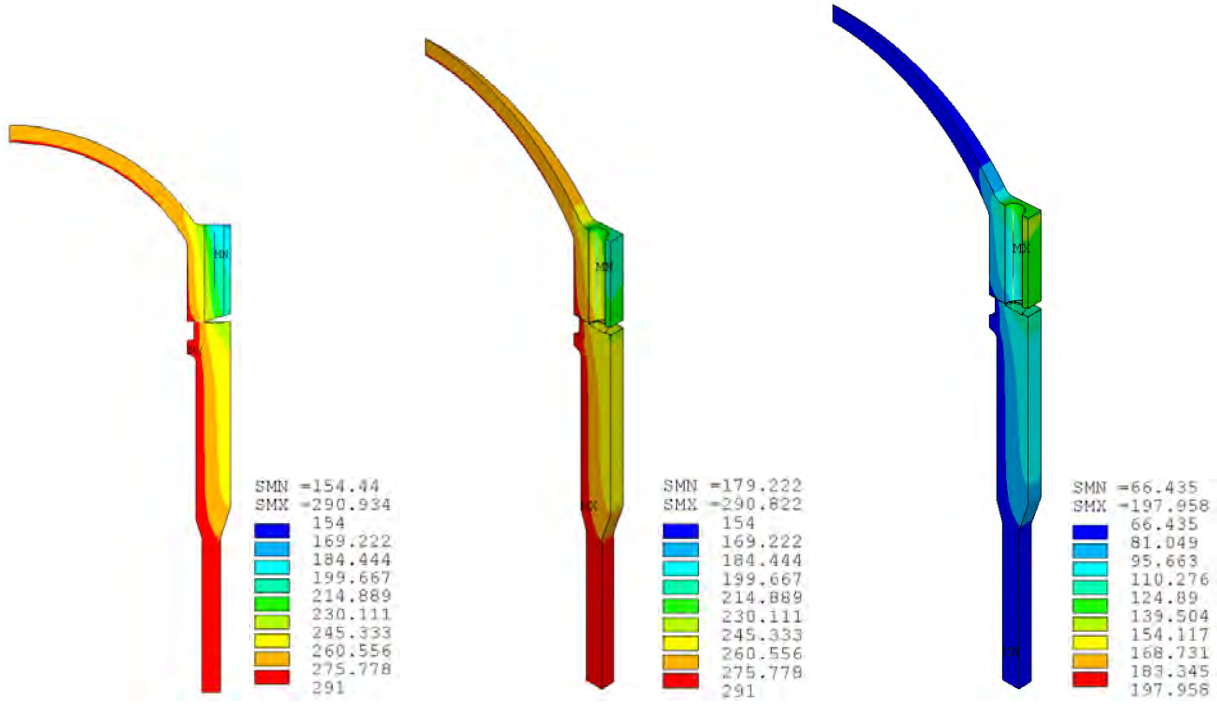

Figure 4. Temperature distribution [°C] during start-up (left: 2D, center: 3D) and shutdown (right: 3D).

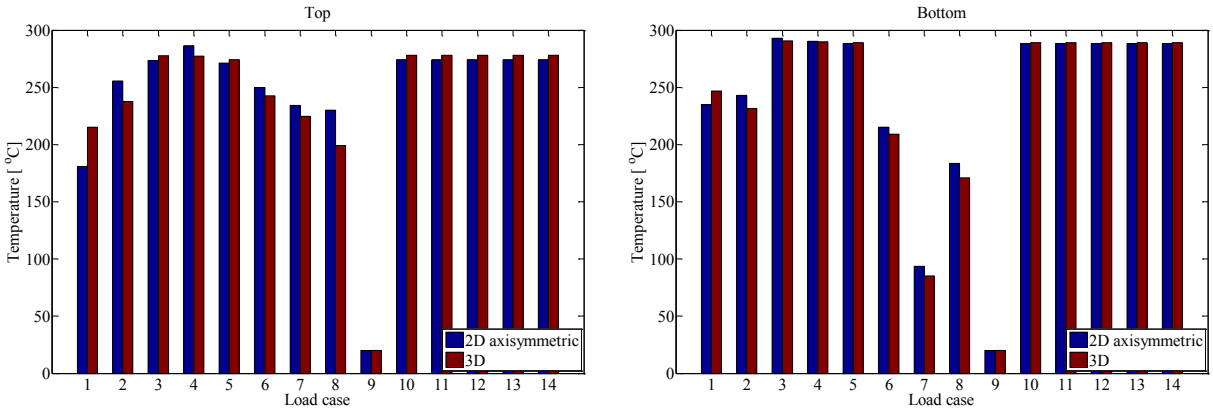

Figure 5. Temperature in the bolts.

Stress Distribution

Figure 6 shows the stresses in the bolts during the different load cases. The results are shown for two different locations: the top and bottom of the bolts (see Figure 1). In most cases, the stresses calculated with the 3D model are slightly smaller than the stresses resulting from the 2D axisymmetric model. This can be explained by the temperature distributions as shown in Figure 4. Due to the difference in modeling of the bolt hole, the temperature gradient over the wall of the flanges is slightly smaller in the 3D model. This leads to smaller deformations and smaller thermal stresses. Another difference between the two mechanical models is that in the 2D axisymmetric model, the bolt force is circumferentially uniformly distributed over the flanges. In the 3D model, the bolt forces act locally.

The stresses at inside of the upper part of the bolt fluctuate much more that the stresses at the outside of the upper part (see Figure 6). At the lower part of the bolt, it is the other way around. This will be explained below.

In Figure 7 the deformed shape of the flanges and the stresses in the bolt are shown for start-up and shutdown. The maximum stresses are in the upper and lower parts of the bolt. The stresses in the bolts consist of a membrane stress and a bending stress. The membrane stress is constant and the bending stress varies over the length and cross-section of the bolt. At one side of the cross-section, the total stress is equal to the membrane stress plus the bending stress. At the other side of the cross-section, the total stress is equal to the membrane stress minus the bending stress. During an increasing temperature transient (e.g. start-up), the inner wall of the vessel is hot and the outer wall of the vessel is cold. During a decreasing temperature transient (e.g. shutdown), the inner wall of the vessel is cold and the outer wall of the vessel is hot. This leads to different bending shapes of the flanges and the bolts (see Figure 7).

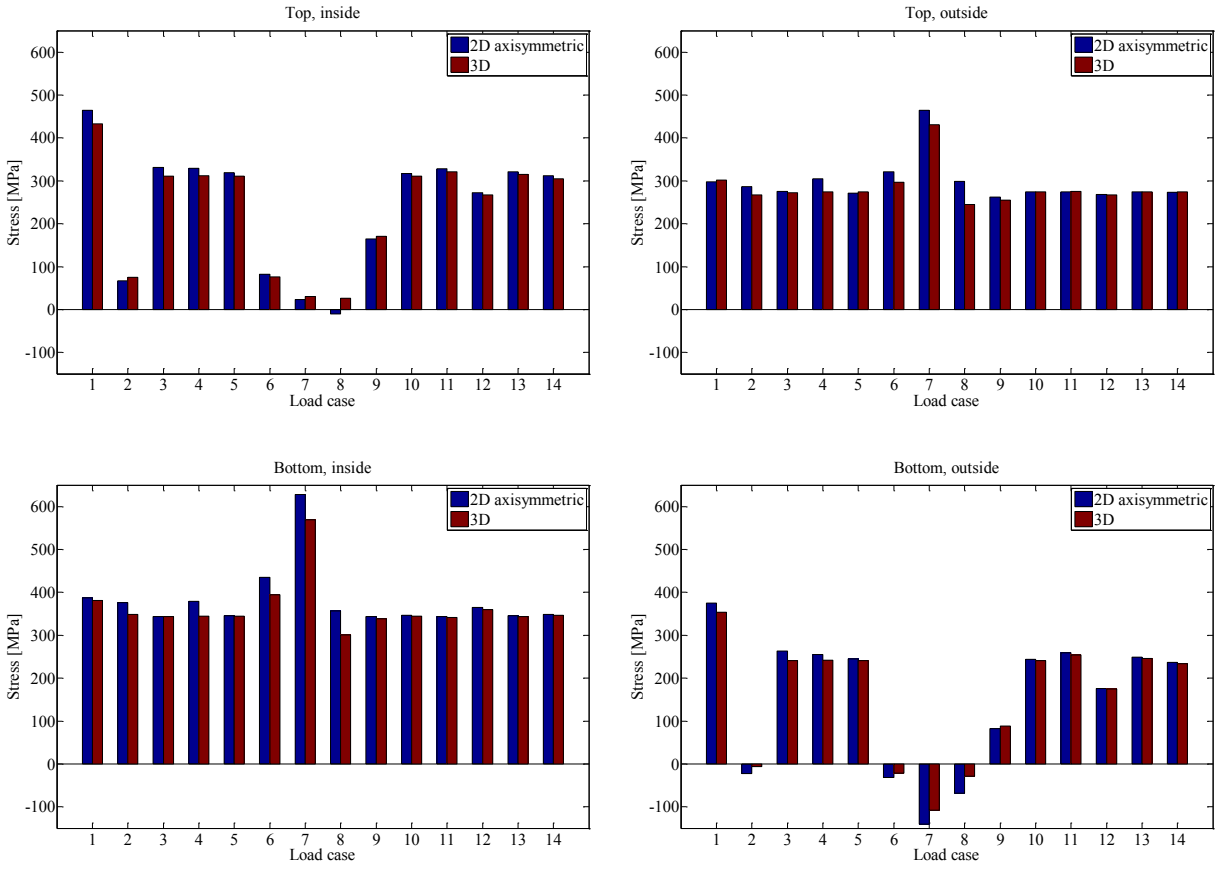

Figure 6. Stress in the bolts.

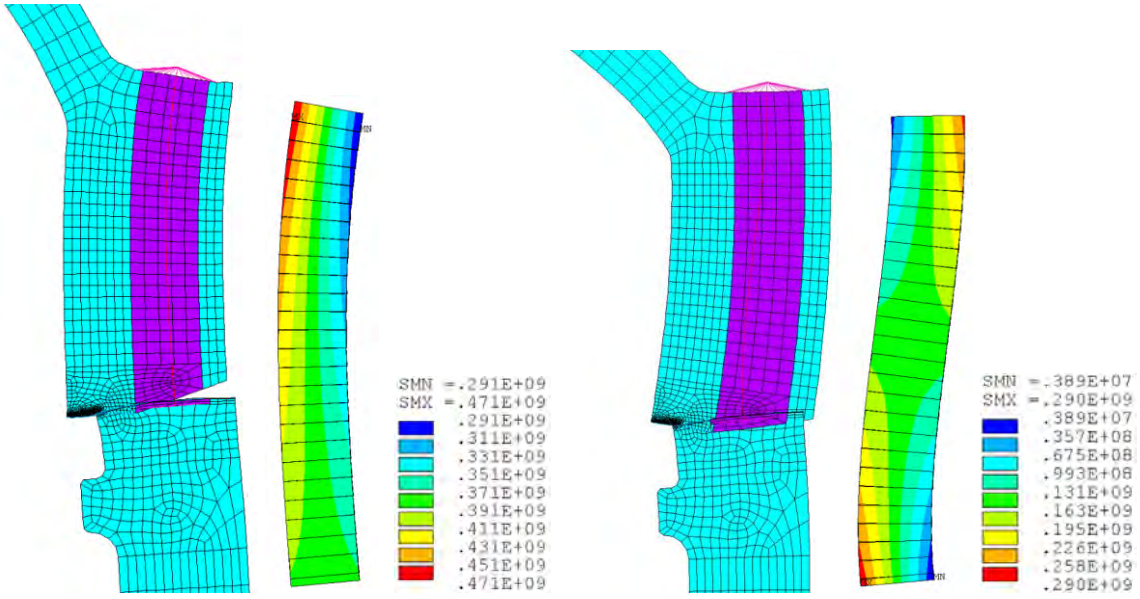

Figure 7. Deformation in flanges and bolt (100 times scaled up) and stress distribution in bolt [MPa] (expanded view) during start-up (left) and shutdown (right) – 2D axisymmetric model.

During the increasing temperature transient (load case 1), the membrane stress is larger than during the decreasing temperature transients (load cases 2, 5-8). In the last case, the values of the bending stresses have the same order of magnitude as the membrane stresses. In the first case, the bending stress is considerably smaller than the membrane stress. This is schematically depicted in Figure 8. The figure clearly illustrates that the largest stress fluctuations are observed at the inside of the upper part of the bolt and the outside of the lower part of the bolt.

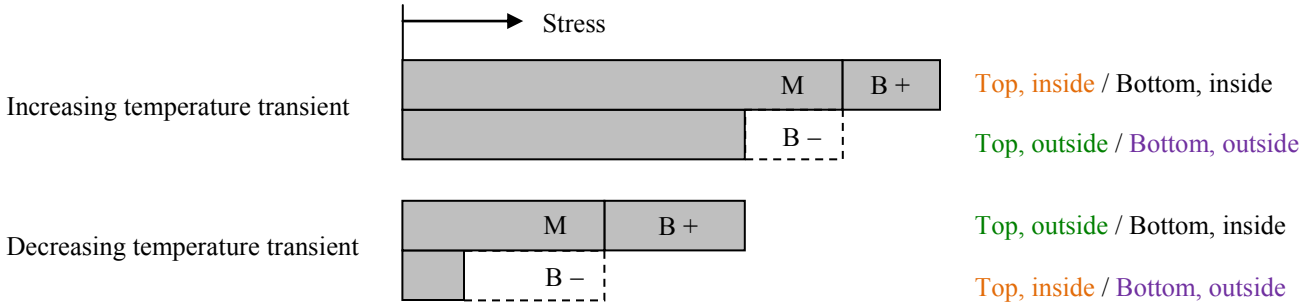

Figure 8. Schematic representation of stress in the bolts.

Cumulative Usage Factor

The CUFs resulting from the 2D axisymmetric and the 3D analyses are summarized in Table 5. At each location, a usage factor was calculated for the inside and outside of the bolt (see Figure 1). The results obtained with the 3D model are slightly lower than the results obtained with the 2D axisymmetric model. This corresponds with the trend that was seen in the calculation of the stresses.

Table 5: CUFs of bolts for different locations at bolts.

Location	Description	CUF 2D Axisymmetric	CUF 3D
1	Top, inside	0.52	0.43
2	Top, outside	0.10	0.10
3	Bottom, inside	0.17	0.16
4	Bottom, outside	0.49	0.40

In both models, the largest CUF is at the inside of the upper part of the bolt. At the lower part of the bolt, the largest CUF is found at the outside. The locations of these maxima can be explained by the fact that at these locations the largest stresses fluctuations occur (see previous section).

CONCLUSIONS

In this paper, the influence of 2D and 3D modeling of the flanges of the RPV on the fatigue assessment of the bolts is presented. The CUFs calculated with the 3D model are slightly lower than the CUFs calculated with the 2D axisymmetric model. However, the values show the same trends. In all cases, there is a considerable difference between the CUFs of the bolt at the inner side and at the outer side of the vessel. Rotation of the bolts during the operation period of the NPP could lead to a more even distribution of the cyclic loadings and lower maximum CUFs.

REFERENCES

Kim, J., Yoon, J.-C., and Kang, B.-S. (2007). "Finite element analysis and modeling of structure with bolted joints," *Applied Mathematical Modelling*, 31, 895-911.

KTA (1996). *KTA 3201.2 (06/96), Components of the Reactor Coolant Pressure Boundary of Light Water Reactors; Part 2: Design and Analysis,* Safety Standards of the Nuclear Safety Standards Commission (KTA).

Safety Report Series No. 57 (2008). *Safe Long Term Operation of Nuclear Power Plants*, Safety Report Series No. 57, International Atomic Energy Agency, Vienna.

Wärmeatlas (1984). *VDI-Wärmeatlas; Berechnungsblätter für den Wärmeübergang, 4th ed.,* VDI-Verlag.